A robust pipeline for the systematic validation of sRNA effectors suggests cross-kingdom communication in the symbiosis of *Serendipita indica* with *Arabidopsis thaliana*

Sabrine Nasfi, Saba Shahbazi, Katharina Bitterlich, Ena Šečić, Karl-Heinz Kogel & Jens Steinbrenner

Institute of Phytopathology, Research Centre for BioSystems, Land Use and Nutrition, Justus-Liebig-University Giessen, Heinrich-Buff-Ring 26, 35392 Giessen, Germany.

***Correspondence:**

karl-heinz.kogel@agrar.uni-giessen.de

All E-mail addresses:

Sabrine.Nasfi@agrar.uni-giessen.de (ORCID no.: 0000-0001-5916-0824)

Karl-Heinz.Kogel@agrar.uni-giessen.de (ORCID no.: 0000-0003-1226-003X)

Jens.Steinbrenner@gmail.com (ORCID no.: 0000-0003-1008-2268)

Ena.Secic@agrar.uni-giessen.de (ORCID no.: 0000-0002-6469-4895)

Shahbazi.saba@yahoo.com (ORCID no.: 0009-0005-9222-3715)

katha.bitterlich@gmail.com (ORCID no.: 0009-0003-5976-1322)

Abstract

Cross-kingdom RNA interference (ckRNAi), the bidirectional communication between microbes and their host counterparts, is a key element in the outcome of host colonization. Whether mutualistic fungi of the Serendipitaceae family with their broad host range use small RNA effectors (sRNAs) to colonize plant roots is still under debate. To investigate if ckRNAi is a factor in the symbiosis of *Serendipita indica* (*Si*) with *Arabidopsis thaliana* (*Ath*), we established a pipeline to validate expression, translocation and post-transcriptional gene silencing of host genes by *Si*-derived sRNAs (*Si*sRNAs). First, we confirmed the expression of *Si*sRNAs both in axenic fungal culture and during *Ath* root colonization using stem-loop PCR. Then, to verify the translocation of putative *Si*sRNA effectors, an ARGONAUTE 1 immuno-purification assay (*At*AGO1-IP) was employed, detecting fungal *Si*sRNAs being loaded into the plant RNAi machinery in *Si*-colonised roots. Subsequently, *Si*sRNAs and artificial sRNAs (amiRNAs), were transiently expressed in *Ath* protoplasts to test their gene silencing activity. Stem-loop PCR confirmed expression of sRNA effectors and qPCR validated post-transcriptional gene silencing of their predicted target genes involved in cell wall organization, hormonal signalling regulation, plant immunity and gene expression. Moreover, 5’-RLM-RACE analysis revealed amiRNA-mediated canonical cleavage in *Arabidopsis* targets. In conclusion, this study provides a blueprint for rapid selection and analysis of sRNA effectors in plant-microbe interactions in general and suggests cross-kingdom communication in the Sebacinoid symbiosis.

Keywords

Arabidopsis, AGO1-IP, cross-kingdom communication, *Serendipita indica,* sRNA effectors, symbiosis, 5'-RLM-RACE, RNA interference

Introduction

RNA interference (RNAi) is a regulatory process in most eukaryotes in which gene expression is silenced at the transcriptional or post-transcriptional level by the action of small (s) RNA and is associated with the control of genome stability, developmental processes, and responses to biotic and abiotic stresses (Zhan and Meyers, 2023). Two types of sRNAs predominate in plants: Micro (mi) RNAs are 20-22 nucleotides (nt) in length processed from primary miRNAs (pri-miRNAs) containing a stem-loop structure encoded by microRNA (*MIR)* genes (Meyers and Axtell, 2019; Reinhart *et al.,* 2002). In contrast, small-interfering (si) RNAs are RNA molecules of 20-24 nt in length produced from longer endogenous RNA templates or from exogenous RNA sequences (viruses or transgenes). miRNA and siRNA precursors are processed by RNase III-like endonucleases named DICER-like (DCL), then bound by ARGONAUTE (AGO) proteins, which are incorporated into the RNA-Induced Silencing Complex (RISC), where they target complementary mRNA transcripts to induce post-transcriptional gene silencing (PTGS) (Iwakawa & Tomari, 2022). In addition to the involvement in intracellular RNAi, plant sRNAs can move intercellularly across plasmodesmata and systemically across the phloem and thus act cell non-autonomous and can also move between interacting species. In the latter case, sRNA effectors are transferred bidirectionally between plant hosts and pathogenic microbes to modulate defence and virulence, a phenomenon called cross-kingdom RNAi (ckRNAi) (Göhre and Weiberg, 2023; Mahanty *et al*., 2023; Wang *et al*., 2017). ckRNAi in plant-pathogen interactions was discovered in 2013 when the necrotrophic fungus *Botrytis cinerea* was shown to induce silencing of host defence genes in *Solanum lycopersicum* and *Arabidopsis thaliana* (*Ath*) (Weiberg *et al.,* 2013). Since then, several reports supported the existence of ckRNAi (Derbyshire *et al.,* 2019; Wang *et al.,* 2016) and showed that sRNA effectors exchange can be bidirectional (Zhang *et al.,* 2016).

Already in 2006, Huang and colleagues reported reduced nematode infectivity when root-knot nematodes (RKN) fed on roots of Arabidopsis plants expressing double-stranded (ds) RNA targeting the *16D10* gene, which encodes a conserved

secretory RKN root growth-stimulating peptide known to be involved in parasitism (Huang *et al.,* 2006). Later, it was shown that sRNA can indeed move from a plant to an attacking pathogen in the interaction of barley and wheat with the powdery mildew fungus (*Blumeria graminis*) (Nowara *et al.,* 2010). Transient transformation with a plasmid overexpressing dsRNA directed against the fungal *AVR10* gene increased the susceptibility of leaf epidermal cells to the corresponding *Blumeria graminis* races, a technique termed host-induced-gene-silencing (HIGS). Since then, numerous reports have shown that HIGS is an efficient strategy for pests and disease control in crops (Cai et al., 2018; Koch et al., 2013; Liu et al., 2020; Sang & Kim, 2020; Zand Karimi & Innes, 2022).

Although ckRNAi and related artificial processes such as HIGS were discovered in plants more than 10 years ago, the molecular mechanisms are still not fully understood. For instance, the mode of bidirectional transfer of RNAs in extracellular vesicles (EVs) is still a matter of debate (He, Cai, *et al.,* 2021; He, Hamby, *et al.,* 2021; Nasfi & Kogel, 2022; Rutter & Innes, 2018), and the occurrence in mutualistic symbioses is little researched but an increasing number of studies are shedding the light on ckRNAi in plant-symbiont interactions (Qiao *et al.,* 2023).

ckRNAi in mycorrhizal symbioses seems to include miRNA and transfer RNA fragments (tRFs). For example, Pmic_miR-8, a miRNA from ectomycorrhizal fungus *Pisolithus microcarpus* enhanced the colonization of its host *Eucalyptus grandis and* thus plays a role in the beneficial ectomycorrhizal symbiosis (Wong-Bajracharya *et al.,* 2022). In addition, recent *in silico* analysis of the sRNA population from *Rhizophagus irregularis*, supported by degradome data from *Medicago truncatula*, has shown that some sRNAs of Rhizophagus modulate root colonization (Silvestri *et al.,* 2019). Moreover, tRFs identified in root nodule symbioses between soybean and the bacterial symbiont *Bradyrhizobium japonicum* hijack *Glycine max* AGO1 and are positive regulators of rhizobial infection and nodule formation (Ren *et al.,* 2019), further emphasising the existence of ckRNAi in plant-mutual interactions.

107 Key to understanding ckRNAi is the identification and functional validation of sRNA
108 effectors, and tools are needed to study the mode of action of numerous sRNAs
109 derived from extensive sRNA sequencing data. Here, we report on a pipeline for
110 sRNA effectors validation by studying the interaction between the mutualistic
111 basidiomycete fungus *Serendipita indica* (*Si*) and the dicot model plant *Ath*. *Si* was
112 originally isolated from the roots of the shrubs *Prosopis juliflora* and *Ziziphus*
113 *nummularia* in the Indian Thar desert (Verma *et al.,* 1998). The beneficial activity of
114 the fungus includes plant growth promotion, plant resistance priming, enhanced
115 nitrate and phosphate delivery, promotion of adventitious root and root hair
116 formation, early flowering, support of higher seed yield, alteration in secondary
117 metabolites, and hardening of tissue cultured plants (Glaeser *et al.,* 2016; Qiang *et*
118 *al.,* 2012; N. Verma *et al.,* 2022; Weiß *et al.,* 2016; Xu *et al.,* 2018; Zuccaro *et al.,*
119 2011). *Si* transfers protein effectors to host cells to exploit the host´s metabolism
120 and promote microbial colonization (Akum *et al.,* 2015; Osborne *et al.,* 2023). To
121 further explore the potential of *Si* we recently demonstrated the global change in
122 sRNA profiles in the interaction of *Si* and the grass model *Brachypodium distachyon*
123 (*Bd*) (Šečić et al., 2021). Among *Bd*- and *Si*-generated sRNAs with putative functions
124 in the interacting organism, we found proteins involved in circadian clock,
125 flowering regulation and immunity as potential targets of putative fungal sRNA
126 effectors.

127 In the present work, we analysed the function of *Si*-derived sRNAs (*Si*sRNAs) in
128 more detail by investigating the interaction between *Si* and *Ath*. By performing an
129 *At*AGO1 immunoprecipitation assay, we confirmed the loading of *Si*sRNA into the
130 RNAi machinery of *Ath*. We developed a functional protoplast assay to validate
131 putative fungal sRNA effectors by testing their gene-silencing activity.
132 Furthermore, we confirmed sRNA transformation and expression in plant
133 protoplasts with stem-loop PCR and recorded downregulation of the
134 corresponding predicted host target genes by qPCR. Finally, we confirmed sRNA
135 effector candidate-mediated degradation of host mRNA by 5'-RLM-RACE. The data

136 support naturally occurring ckRNAi between the mutualistic fungus *Serendipita*
137 *indica* and *Arabidopsis thaliana*.

138

139 **Materials and methods**

140 **Plant material and growth conditions**

141 For protoplast isolation, *Arabidopsis thaliana* plants of ecotype Columbia-0 (Col-0)
142 were cultivated in a 4:1 ratio of T-type soil (F.-E. Typ Nullerde, Hawita) and crystal
143 quartz sand mixture for 4 to 5 weeks in a growth chamber in a 19℃ day/18℃ night
144 (9 h of light, 150 µmol photons m^{-2} s^{-1}) and a constant relative humidity of 60%. For
145 interaction studies of *Ath* roots and *Serendipita indica* (IPAZ-11827, Institute of
146 Phytopathology, Giessen, Germany), plants were grown on vertical square Petri
147 dishes on an ATS medium (Lincoln *et al.,* 1990) without sucrose and supplemented
148 with 4.5 g/L Gelrite (Duchefa #G1101) in a 22°C day/18°C night cycle (8 h of light).
149 Roots of 14-day-old plants were inoculated with 1 mL of a suspension of 500,000
150 chlamydospores/mL in $H_2O_{0.02\%\ Tween\ 20}$ per Petri dish.

151 **Plasmid construct**

152 AtMIR390a distal stem-loop was digested from the pMDC32B-AtMIR390a-B/c
153 vector (Plasmid #51776, https://www.addgene.org, Carbonell *et al.,* 2014) using
154 Fast digest enzymes EcoRI and HindIII (Thermo Fisher Scientific, FD0274 &
155 FD0505). The pUC18-AtMIR390a-B/c construct was generated by ligating the
156 AtMIR390a precursor into the pUC18 vector (plasmid #50004) backbone using T4
157 DNA Ligase (Thermo Fischer Scientific, EL0011). The *RFP* insert was digested from
158 the pBeaconRFP_GR vector (Bargmann & Birnbaum, 2009) using the restriction
159 enzyme NdeI (NEB, R0111S) and further ligated into the NdeI site of the pUC18-
160 AtMIR390a-B/c vector. 75mer oligonucleotides comprising the amiRNAs and
161 *Si*sRNAs sequences were cloned into the BsaI-sites by Golden Gate strategy using
162 BsaI-HF®v2 (NEB, R3733) and T4 DNA Ligase (Thermo Fischer Scientific, EL0011) in
163 a single reaction, replacing the toxic ccdB gene which allows the selection of 75-

164 mer-positive clones. Before cloning 75-mer oligonucleotides, a third BsaI-site in
165 the pUC18 backbone which would interfere with the Golden-Gate cloning was
166 removed by site-directed mutagenesis using Phusion High-Fidelity DNA
167 polymerase (Thermo Fisher Scientific, F553S) and the Fast digest Dpn I
168 endonuclease (Thermo Fisher Scientific, FD1703) as well as custom-designed site-
169 directed mutagenesis primers pUC18-Mut-Fwd and pUC18-Mut-Rev.
170 The artificially designed amiRNAs and *Si*sRNAs and their corresponding predicted
171 targets are listed in Supplemental Tables 1 & 2. 75-mer oligonucleotides for
172 amiRNAs and *Si*sRNAs were designed following the P-SAMS algorithm developed
173 by the James Carrington lab (Fahlgren *et al.,* 2016) available at http://p-
174 sams.carringtonlab.org. Oligonucleotides are listed in Supplemental Table 3. An
175 *in-silico* design of the cloning was performed using Snapgene software
176 (www.snapgene.com) and the final pUC18-AtMIR390a-RFP-sRNA vector map is
177 shown in Supplement Figure 1.
178 **Protoplast transformation**
179 The "Tape-Arabidopsis Sandwich" method was used for protoplast isolation (Wu
180 *et al.,* 2009). The transformation was performed following the transient expression
181 of recombinant genes using the Arabidopsis mesophyll protoplast (TEAMP)
182 approach (Yoo *et al.,* 2007) with minor modifications. Since the transformation of
183 protoplasts was key to all subsequent experiments, we attempted to optimize its
184 efficiency by varying *i.* protoplast concentration (10x 10^4 and 5x 10^4
185 protoplasts/mL), *ii.* plasmid concentration (20 µg, 30 µg, and 40 µg) pUC18-
186 AtMIR390a-RFP-sRNA and *iii*. incubation time (24 and 48 h). High transformation
187 efficiency was reported when using 5x 10^4 protoplasts/ml with a plasmid
188 concentration of 30 µg and an incubation time of 24 h, which was comparable to
189 the reported transformation efficiencies of *Ath* leaf protoplasts (Yoo *et al.,* 2007).
190 Total cell numbers were counted using a Fuchs-Rosenthal counting chamber
191 under a light microscope. A microscopic check of protoplast transformation was
192 done using an epifluorescence microscope (TCS SP2 Leica). Images were acquired

193 with the image software Leica Application Suite (LAS) and all counting was
194 performed in triplicates. Transformed protoplasts were stored at -80°C for further
195 studies.

196 **RNA extraction and quality analysis**

197 Total RNA was extracted from protoplasts using QuickRNA™ Miniprep Kit (Zymo
198 Research, R1050) with an on-column DNase I treatment. Total RNA from *Si-Ath*
199 interaction growing on ATS plates was extracted using Direct-zol RNA Miniprep
200 (Zymo Research, R2051) with an on-column DNase I treatment. The RNA
201 concentration was determined with the NanoDrop ND-1000 Spectrophotometer
202 (Thermo Fisher Scientific, USA) and the purity was determined by measuring
203 A260/280 and A260/230 ratios. The quality of the RNA extracted from transformed
204 protoplasts was checked using the Agilent 2100 Bioanalyzer Nano Chip (Agilent,
205 Germany).

206 **Stem-Loop-RT-End-PCR**

207 *Si*sRNAs and the designed amiRNAs were used as templates to design specific
208 stem-loop (SL) primers matching the corresponding sRNA over six nt at the 3´ end.
209 Hairpin primers (cDNAhp) and forward primers were designed using the tool
210 published in Adhikari et al (2013) based on Varkonyi-Gasic et al., (2007) (Adhikari
211 *et al.,* 2013; Varkonyi-Gasic & Hellens, 2011). Stem-loop PCR was performed as
212 described by Werner et al., (2021) (Werner *et al.,* 2021). End-point PCR was used to
213 assess the expression of *Si*sRNAs and amiRNAs. The PCR program was optimized
214 to 95 °C for 5 min; followed by 40 cycles of 95 C for 30 s, 60°C for 30 s, 72°C for 30
215 s; and 72°C for 5 min and then held at 4 °C. PCR products were separated and
216 visualized in 2 % TBE -agarose gels. Stem-loop PCR primers are listed in
217 Supplemental Table 4.

218 **AGO-IP**

219 To perform AGO1 immunoprecipitation, 5 g of *Si* mycelium or *Ath* roots inoculated
220 with *Si* were ground to a fine powder using a precooled mortar and pestle. Co-
221 immunoprecipitation, sRNA recovery, and western blot analysis were performed

222 as described in the publication of Dunker et *al.,* 2021. Anti-AGO1 polyclonal
223 antibody (Agrisera, AS09 527) and IRDye® 800CW Goat anti-Rabbit IgG Secondary
224 Antibody (LI-COR, 926-32211) were used.

225 **PTGS detection by qPCR**

226 The standard curve method was used to test the efficiency of the qPCR transcript
227 primers using a serial dilution of *Ath* cDNA library along with 3 different primer
228 concentrations (0.4 µM, 0.2 µM and 0.1 µM for each primer) and 5 µL of SybrGreen
229 (Sigma-Aldrich). The total volume of 10 µL and three technical replicates are
230 considered for each reaction. Before master mix preparation, 2 µL ROX (CRX
231 reference dye, Promega, C5411) were added to 1 mL SybrGreen as a passive
232 reference dye that allows fluorescent normalization for qPCR data. For the
233 preparation of cDNA first strands, 500 ng of RNA samples from transformed *Ath*
234 protoplasts and control protoplasts were used. qPCR was performed using the
235 QuantStudio 5 Real-Time PCR system (Applied Biosystems) in the 384-well plate as
236 follows: 50°C for 2 min, 95°C for 10 min, followed by 40 cycles of 95°C for 15 s, and
237 60°C for 1 min, with an additional melt curve stage consisting of 15 s at 95°C, 1
238 min at 60°C, and 15 s at 95°C.

239 To evaluate the relative quantification of *Ath* transcripts by qPCR, the level of gene
240 expression was standardized to the control protoplasts. Fold change of *ΔΔ*ct values
241 and standard errors were calculated for all mean values. All qPCR primers are
242 listed in Supplemental Table 5.

243 **5´-RLM-RACE**

244 RNA ligase-mediated rapid amplification of cDNA ends (5´-RLM-RACE) was
245 performed using FirstChoice® RLM-RACE kit (Thermo Fisher Scientific) following
246 the manufacturer protocol and omitting the dephosphorylation and decapping
247 steps. One µg of RNA isolated from *At*h protoplasts and control protoplasts were
248 used as a template and ligated to the 5´-RACE adapter using T4 RNA Ligase [10
249 U/µL] (Thermo Fisher Scientific). The ligation reaction was used entirely to
250 generate the first cDNA strand. Two rounds of nested hot-start touch-down PCR

251 were performed using outer (first) and inner (second) 5´-RLM-RACE universal
252 primers in combination consecutively with gene outer specific and gene inner
253 specific primers. PCR products were evaluated in a 1.5% agarose gel and bands of
254 the expected size were excised. Products were cleaned with the Wizard® SV Gel
255 and PCR Clean-Up System (Promega) and cloned with the pGEM®-T Vector Systems
256 (Promega). For each band, six clones were selected for sequencing at LGC
257 genomics. The oligonucleotides used are listed in the Supplemental Table 6.

258 **T-vector cloning and sequencing**

259 Stem-loop PCR and 5´-RLM-RACE PCR amplification products were purified using
260 The Wizard® SV Gel and PCR Clean-Up System (Promega). Cloning of the different
261 PCR products was performed as described in the pGEM®-T Vector system
262 according to the instructor´s instructions (Promega). Sequencing was performed
263 at LGC Genomics (Berlin, Germany) and analysed using the Snapgene tool (GSL
264 Biotech, available at snapgene.com). All PCR primers are presented in
265 Supplemental Table 7.

266 **Statistics Analysis**

267 To assess the downregulation of *Ath* genes via qPCR, the 2−ΔΔCt method was used
268 for the quantification of *Ath* target transcript. The results are expressed as values
269 of the fold change of the transcript expression level in comparison to the control
270 and compared using a two-sided paired student t-test. Data showed a normal
271 distribution in the Shapiro-Wilk test or D´Agostino & Pearson test.

272

273 **Results**

274 We developed a pipeline for the systematic validation of sRNA effectors in the
275 mutualistic interaction of *Serendipita indica* and *Arabidopsis thaliana*, comprising i.
276 detection of fungal sRNAs (*Si*sRNAs) in axenic culture and *Si*-colonized *Ath* roots, ii.
277 detection of the association of *Si*sRNAs with the *At*AGO1 protein, and iii. validation
278 of the gene silencing activity of *Si*sRNAs in *Ath* protoplasts (Figure 1).

279

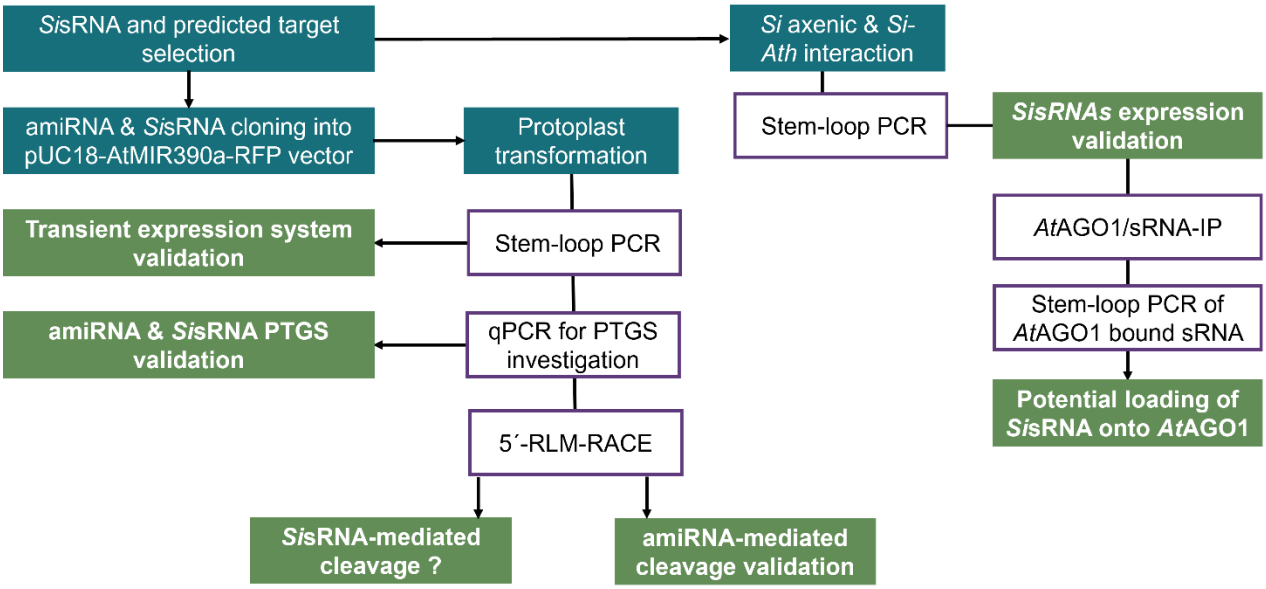

Figure 1. Schematic flowchart showing the molecular methods and outputs in this study. The turquoise colour indicates the different input material and purple indicates the wet-lab steps. Green represents the validated outputs of the study. For details also see Material and Methods. *Si*, *Serendipita indica*; *Ath*, *Arabidopsis thaliana*; PTGS, post-transcriptional gene silencing; amiRNA, artificial miRNA.

*Si*sRNAs are present in axenic cultures of *Serendipita indica*

In a previous RNAseq study, we identified potential fungal sRNA effectors in axenic *Si* cultures and *Si*-colonised *Brachypodium distachyon* roots (Šečić *et al.,* 2021). Here we further investigated a set of 15 putative *Si*sRNA effector candidates by focusing on 21 nt sRNAs encompassing all four 5'-terminal nucleotides: adenine (A), uracil (U), cytosine (C) and guanine (G) (Supplementary Table 8). We used multiplexed stem-loop PCR as a specific and sensitive method to amplify sRNAs followed by gel electrophoresis and showed that all 15 *Si*sRNAs could be amplified from 4-week-old axenic *Si* culture (Figure 2). Next, we cloned a subset of *Si*sRNAs (*Si*sRNA21, *Si*sRNA23, *Si*sRNA24, *Si*sRNA28, *Si*sRNA154 and *Si*sRNA296) and subjected them to Sanger sequencing, which further confirmed the expected *Si*sRNA sequences.

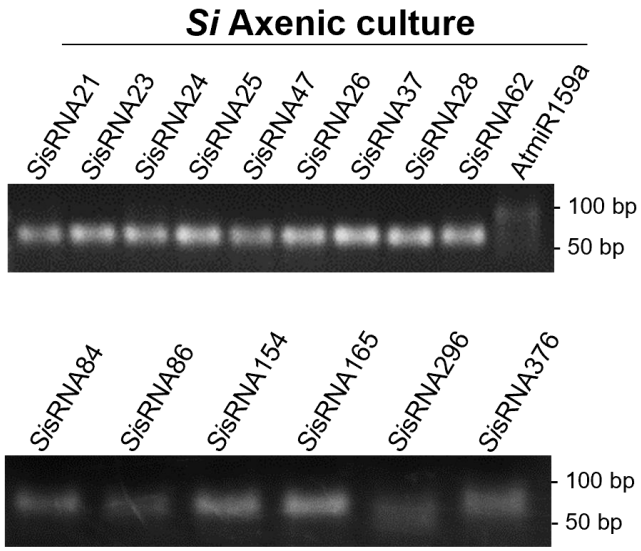

Figure 2: Stem-loop PCR analysis of *Si*sRNA detected in axenic cultures of *Serendipita indica*. Multiplexed stem-loop PCR confirmed the presence of *Si*sRNAs in a 4-week-old *Si* axenic culture. A PCR product of the expected size of 62 bp (sum of the 21 bp of the sRNA sequence, loop region, plus the forward primer and the reverse primer length) is visualized in a 2% agarose gel. The plant AtmiR159a which served as a negative control was not detected.

_Si_sRNAs are present in colonized _Arabidopsis thaliana_ roots

Next, we analysed the presence of nine *Si*sRNAs (*Si*sRNA21, *Si*sRNA23, *Si*sRNA24, *Si*sRNA25, *Si*sRNA26, *Si*sRNA28, *Si*sRNA37, *Si*sRNA47, and *Si*sRNA62) (Supplemental Table 8) in *Si*-colonized *Ath* roots. Roots of 14-day-old seedlings were inoculated with *Si* chlamydospores and harvested at 3-, 7-, and 14 days post-inoculation (dpi). Fungal colonization of roots was confirmed after 7 days both by confocal laser scanning microscopy (CLSM) using the chitin-specific dye Wheat Germ Agglutinin with Alexa Fluor 488 (WGA-AF-488) (Figure 3 A) and by PCR using both specific *ITS* gene primers and *Si*-specific *Ubiquitin* primers (Supplemental Figure 2). Multiplexed stem-loop PCR of total RNA extracted from *Si*-colonized *Ath* roots at different time points detected eight out of the nine selected *Si*sRNAs (Figure 3 B-D). Bands for *Si*sRNA21 and *Si*sRNA24 did not consistently show up at all three-

320 time points, likely because of the limitations associated with multiplexing the
321 hairpin cDNA primers (Colombo *et al.,* 2013; Kramer, 2011; Varkonyi-Gasic and
322 Hellens, 2011). Consistent with this notion, we detected the expression of
323 *Si*sRNA21 and *Si*sRNA24 at 7 dpi in a stem-loop PCR with less multiplexing
324 (Supplemental Figure 3). A subset of three *Si*sRNAs (*Si*sRNA21, *Si*sRNA24,
325 *Si*sRNA28) were cloned and submitted for Sanger sequencing, confirming the
326 expected *Si*sRNA sequences in *Si*-colonized *Ath* roots.

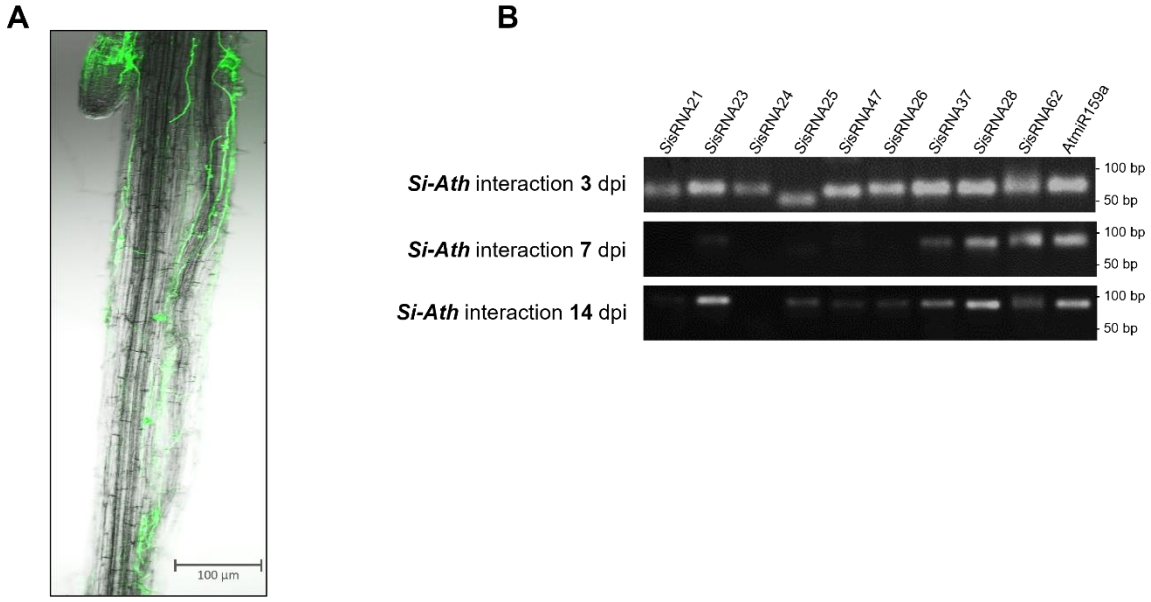

327

328 **Figure 3: Arabidopsis roots colonized by *Serendipita indica* and gel analysis of**
329 ***Si*sRNAs in the *Si-Ath* interaction**. **(A)** Root colonization pattern at 7 dpi.
330 Fluorescence microscopy shows green chitin-specific WGA-AF488 staining of *Si*
331 hyphal walls (λexc494 nm, λem515) **(B)** Detection of *Si*sRNAs in roots at 3-, 7- and
332 14 dpi using multiplexed stem-loop PCR. Agarose gel analysis of *Si*sRNA detected
333 bands of the expected size of 62 bp. Plant AtmiR159a was used as a positive
334 control for a plant-expressed sRNA.

335

336 ***Si*sRNAs are loaded onto Arabidopsis AGO1**

337 To further substantiate the hypothesis that ckRNAi occurs in the interaction
338 between *Si* and *Ath* and that *Si*sRNAs are likely to be loaded into the Arabidopsis
339 RISC complex, we conducted *At*AGO1/sRNA co-immunopurification (Co-IP) using

340 samples of *Si*-colonised roots, followed by stem-loop PCR analysis (Carbonell,
341 2017b; Dunker *et al.,* 2021). To exclude the possibility that the *Ath*-specific anti-
342 AGO1 antibody would cross-react with fungal AGOs, we first performed an
343 *At*AGO1/sRNA Co-IP using a 4-week-old *Si* axenic culture, followed by Western-Blot
344 (WB) analysis. No binding of the *At*AGO1-specific antibody was detected in samples
345 from *Si* axenic cultures confirming the specificity of the plant anti-AGO1 antibody
346 (Supplementary Figure 4A). In line with this, no *Si*sRNAs could be detected by stem-
347 loop PCR using *Si*sRNA-specific stem-loop primers (Supplementary Figure 4B).
348 Next, we performed *At*AGO1/sRNA Co-IP on samples from *Si*-colonized roots (*Si-*
349 *Ath* Co-IP). *Si*sRNA21, *Si*sRNA23, *Si*sRNA24, *Si*sRNA28 and the *At*AGO1-bound
350 AtmiR159a were detected by stem-loop PCR (Figure 4), whereas AtmiR393a*,
351 which is known to preferably bind *At*AGO2 (Mi *et al.,* 2008), was undetectable.
352 Stem-loop PCR products from the *Si-Ath* Co-IP fraction were cloned and
353 sequenced. The sequencing results confirmed the presence of plant AtmiR159a as
354 well as *Si*sRNA2*4* and *Si*sRNA28 with the exact same sequences detected from *Si*
355 axenic cultures and *Si*-colonized *Ath* roots. In addition, two *Si*sRNAs with almost
356 identical sequences to *Si*sRNA21 and *Si*sRNA23 were also co-immunoprecipitated
357 (Supplementary Table 9). These results show that detected *Si*sRNAs are bound to
358 *At*AGO1, supporting the notion that *Si*sRNAs are transferred into *Ath* root cells
359 during root colonisation and loaded into the plant RNAi machinery.

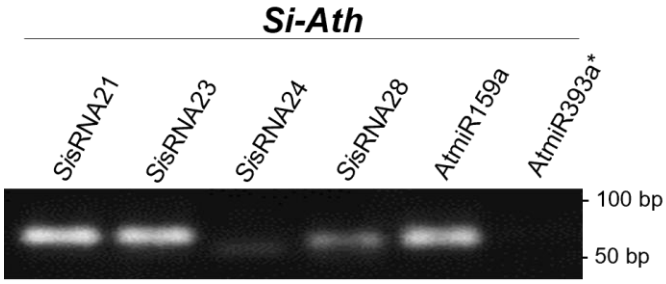

360

361 **Figure 4: *Si*sRNAs co-immunoprecipitated with *At*AGO1 in *Si*-colonized**
362 **Arabidopsis roots.** Stem-loop PCR analysed in agarose gel confirms the presence

363 of *Si*sRNA21, *Si*sRNA23 *Si*sRNA24, *Si*sRNA28, as well as AGO1 bound AtmiR159a but
364 not AGO2 bound AtmiR393a* in AGO1-co-IP samples from *Si*-colonized *Ath* roots.

365

366 **_Si_sRNAs mediate PTGS in transformed Arabidopsis protoplasts**

367 Next, we transiently transformed protoplasts with *Si*sRNAs to demonstrate their
368 gene-silencing activity. *Ath* protoplasts were transformed with a *35S::AtMIR390a*
369 expression construct containing *Si*sRNA21, *Si*sRNA24, *Si*sRNA28 and *Si*sRNA154
370 (confirmed in *Si* axenic culture). Information on these *Si*sRNAs, including their
371 predicted *Ath* target genes, their target predicted scores (TPS), indicating the
372 degree of mismatches with the predicted *Ath* target sequence, their 5'-terminal
373 nucleotides and an alignment to their corresponding target fragment are shown
374 in Supplemental Table 1. We achieved a transformation efficiency of 65% to 90%,
375 calculated as the ratio between the red fluorescing protoplasts and the total
376 number of viable protoplasts (Supplemental Figure 5). Duplexed stem-loop PCR
377 confirmed the expression of the four *Si*sRNAs. All four *Si*sRNAs were successfully
378 amplified (Figure 5). The amplification products were cloned into the pGEM-T®
379 cloning vector and sequencing confirmed their identity.

380

381

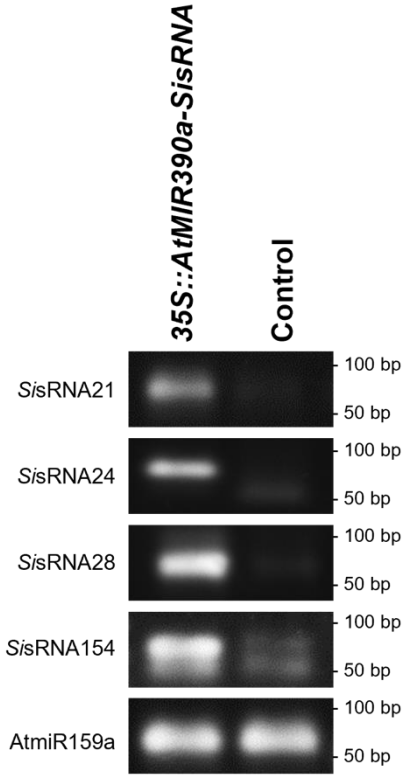

382

383 **Figure 5. Duplexed stem-loop PCR confirming expression of *Si*sRNAs in**
384 **Arabidopsis protoplasts.** Agarose gel analysis of stem-loop PCR confirmed the
385 detection of all four expressed *Si*sRNA in transformed protoplasts 24 hours post-
386 transformation (hpt), but not in control protoplasts. Plant AtmiR159a was used as
387 a positive control.

388

389 Next, we investigated the ability of the expressed *Si*sRNAs to induce PTGS of
390 predicted target genes in protoplasts. *Si*sRNA24 was predicted to target five *Ath*
391 genes: *AT1G57590 (PECTIN ACETYESTERASE 2)* involved in cell wall organization,
392 *AT1G63180 (UDP-D-GALACTOSE 4-EPIMERASE 3)* involved in pollen development,
393 *AT1G65090 (SEED LIPID DROPLET PROTEIN1*) involved in lipid droplet-plasma
394 membrane tethering, *AT4G15765 (FAD/NAD(P)-binding oxidoreductase family*
395 *protein)* involved in jasmonic acid-mediated signalling, and *AT5G16680* (PAIPP2,
396 PHD2) involved in regulation of gene expression (see Supplemental Table 1).

397 Expression of *Si*sRNA24, which has U at the 5'-terminus, and thus a preference for
398 AGO1 (Mi *et al.*, 2008; Montgomery *et al.*, 2008; Takeda *et al.*, 2008), significantly
399 reduced the mRNA abundance of *AT1G63180*, *AT1G65090*, *AT4G15765* and
400 *AT5G16680* in protoplasts 24 h after transformation by 63%, 56%, 45%, and 73%,
401 respectively, (Figure 6 B). Similarly, *Si*sRNA154, also with 5´ U, is predicted to target
402 *AT2G47600 (MAGNESIUM/PROTON EXCHANGER)* involved in magnesium, iron and
403 zinc ion transport and *AT4G32160 (Phox (PX) domain-containing protein)* involved in
404 signal transduction. Expression of *Si*sRN154 significantly downregulated the
405 accumulation of *AT2G47600* mRNA by 37% but not of *AT4G32160*. (Figure 6 D).
406 *Si*sRNA28 has 5' Adenine (A), therefore a loading preference for AGO2 and AGO4
407 (Mi et al., 2008; Montgomery et al., 2008; Takeda et al., 2008). Consistent with this,
408 expression of *Si*sRNA28 did not result in downregulation of any of the three
409 predicted target genes: *AT1G05180 (AUXIN RESISTANT 1*) involved in auxin-activated
410 signalling pathway and response to cytokinin, *AT5G55930* (*ARABIDOPSIS THALIANA*
411 *OLIGOPEPTIDE TRANSPORTER 1*) an oligopeptide transporter, and *AT3G06670*
412 (*PLATINUM SENSITIVE 2 LIKE*) with a regulatory function in ncRNA processing (Figure
413 6 C). Finally, expression of *Si*sRNA21 with 5' Cytosine (C) and thus a preference for
414 AGO5 (Mi et al., 2008; Montgomery et al., 2008; Takeda et al., 2008) resulted in
415 downregulation of predicted target transcripts *AT5G25350* (*EIN3-BINDING F BOX*
416 *PROTEIN 2*), a negative regulator of the ethylene-activated signalling pathway, and
417 *AT5G37600 (ARABIDOPSIS GLUTAMINE SYNTHASE 1)* involved in nitrate assimilation,
418 by 51%, and 16%, respectively (Figure 6 A).

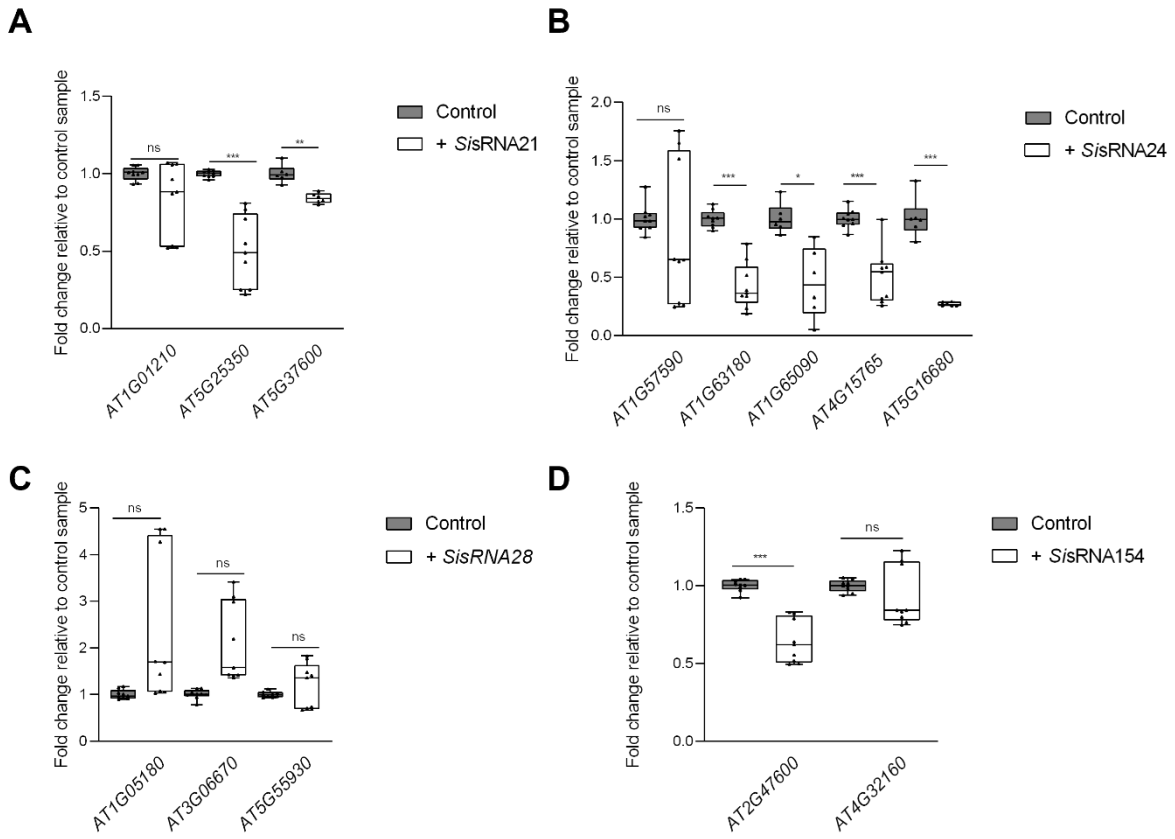

Figure 6. qPCR analysis of target gene silencing in Arabidopsis protoplasts 24 h post transformation with *Si*sRNAs vs. control (protoplast without *Si*sRNA construct). The mRNA transcript levels in transformed protoplasts (+) expressing **(A)** *Si*sRNA21, **(B)** *Si*sRNA24, **(C)** *Si*sRNA28 and **(D)** *Si*sRNA154 normalized against housekeeping gene *Ubiquitin* (*AT3G62250*) are displayed as fold change relative to control protoplasts (-). Data are the average of two to three biological replicates ± standard deviation. Asterisks indicate difference at $p \leq 0.05$(*), $p \leq 0.01$ (**) and $p \leq 0.001$ (***) according to Student's t-test. ns= not significant.

5'-RLM-RACE reveals non-canonical cleavage of Arabidopsis target genes in protoplasts expressing *Si*sRNAs with preference for AGO1

We selected *Si*sRNA24 to study the cleavage pattern of its significantly down-regulated target transcripts *AT1G65090* and *AT4G15765* using RNA-ligase-mediated

433 Rapid Amplification of cDNA Ends (5'-RLM-RACE) (Llave *et al.,* 2002; Ueno *et al.,*
434 2022). For the predicted target transcript *AT1G65090,* no band corresponding to
435 an expected canonical cleavage product was detected (Supplemental Figure 6A)
436 (Carbonell, 2017c; Carthew & Sontheimer, 2009). For target gene *AT4G15765*, we
437 detected a single band of 300 bp in protoplasts expressing *Si*sRNA24*,* which was
438 shorter than the expected size (443 bp), while double bands were observed for the
439 control protoplasts. PCR amplicon from both transformed and control protoplasts
440 were cloned into the pGEM-T® cloning vector and sequenced. Sequence analysis
441 confirmed the alignment of the 300 bp RLM-RACE product with *AT4G15765*.
442 However, it did not confirm the 5´-end position, between nt 10 and 11, predicted
443 for *Si*sRNA24-guided canonical cleavage (Supplemental Figure 6B). However, the
444 absence of cleavage and/or a canonical cleavage product does not exclude the
445 potential of *Si*sRNA24 in mediating predicted *Ath* gene silencing as many previous
446 studies have highlighted the challenge of identifying sRNAs cleavage sites in plants
447 *(Brousse et al.,* 2014; Werner *et al.,* 2021).

448

449 **amiRNAs mediate PTGS in transformed Arabidopsis protoplasts**

450 Working with the naturally occurring *Si*sRNAs can be challenging due to the varying
451 degree of mismatches with their predicted target genes. The position and the
452 significance of these mismatches are crucial factors for PTGS and for the
453 mediation of a canonical target cleavage. To overcome these challenges and to
454 have a proof of concept for the sRNA effector validation pipeline we used
455 artificially designed microRNA (amiRNAs) that, unlike *Si*sRNAs, match their
456 predicted target genes at a higher degree and exhibit a U at their 5´-end. To this
457 end, four amiRNAs were designed: amir21, amir24, amir154, and amir296, cloned
458 into pUC18-AtMIR390a-RFP vector and transformed into *Ath* protoplasts.
459 Subsequently, their expression was confirmed as described for *Si*sRNAs using
460 duplexed stem-loop PCR. Supplemental Table 2 provides information on these
461 amiRNAs, including their predicted *Ath* target genes, their target predicted scores

462 (TPS) indicating the degree of mismatches between the amiRNAs and the *Ath*
463 target sequence, their 5'-terminal nucleotides, and an alignment to their
464 corresponding target fragment. The four amiRNAs were successfully expressed in
465 protoplast (Figure 7), amplification products were cloned into the pGEM-T® cloning
466 vector, and sequencing confirmed amiRNAs sequences.

467

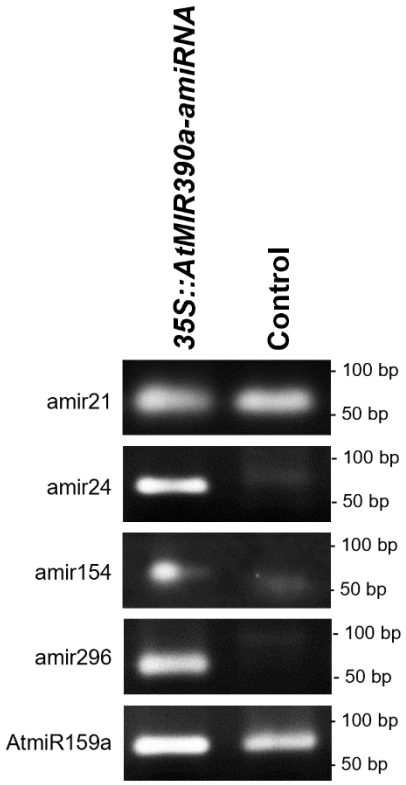

468

469 **Figure 7. Duplexed stem-loop PCR confirming expression of amiRNAs in**
470 **Arabidopsis protoplasts.** Agarose gel analysis of all four expressed amiRNAs in
471 transformed protoplasts 24 hours post-transformation (hpt), but not in control
472 protoplasts. Plant AtmiR159a was used as a positive control.

473

474 The abundance of the four *Ath* transcripts *AT5G25350* (previously investigated for
475 PTGS in protoplasts transformed with *Si*sRNA21), *AT2G39020 (GCN5-RELATED N-*
476 *ACETYLTRANSFERASE 8)* involved in RNA metabolic process, *AT4G32160* (previously
477 investigated for PTGS in protoplasts transformed with *Si*sRNA154), and *AT2G45240*

(METHIONINE AMINOPEPTIDASE 1A) involved in removing the N-terminal methionine from proteins, predicted to be targeted by amir21, amir24, amir154, and amir296, respectively. Target gene expression was quantified 24 h after the transformation of amiRNAs into protoplasts by qPCR. Downregulation of mRNA transcript level was confirmed for *AT5G25350*, *AT2G39020*, *AT4G32160*, and *AT2G45240* by 68%, 43%, 50%, and 65%, respectively, compared to control (Figure 8).

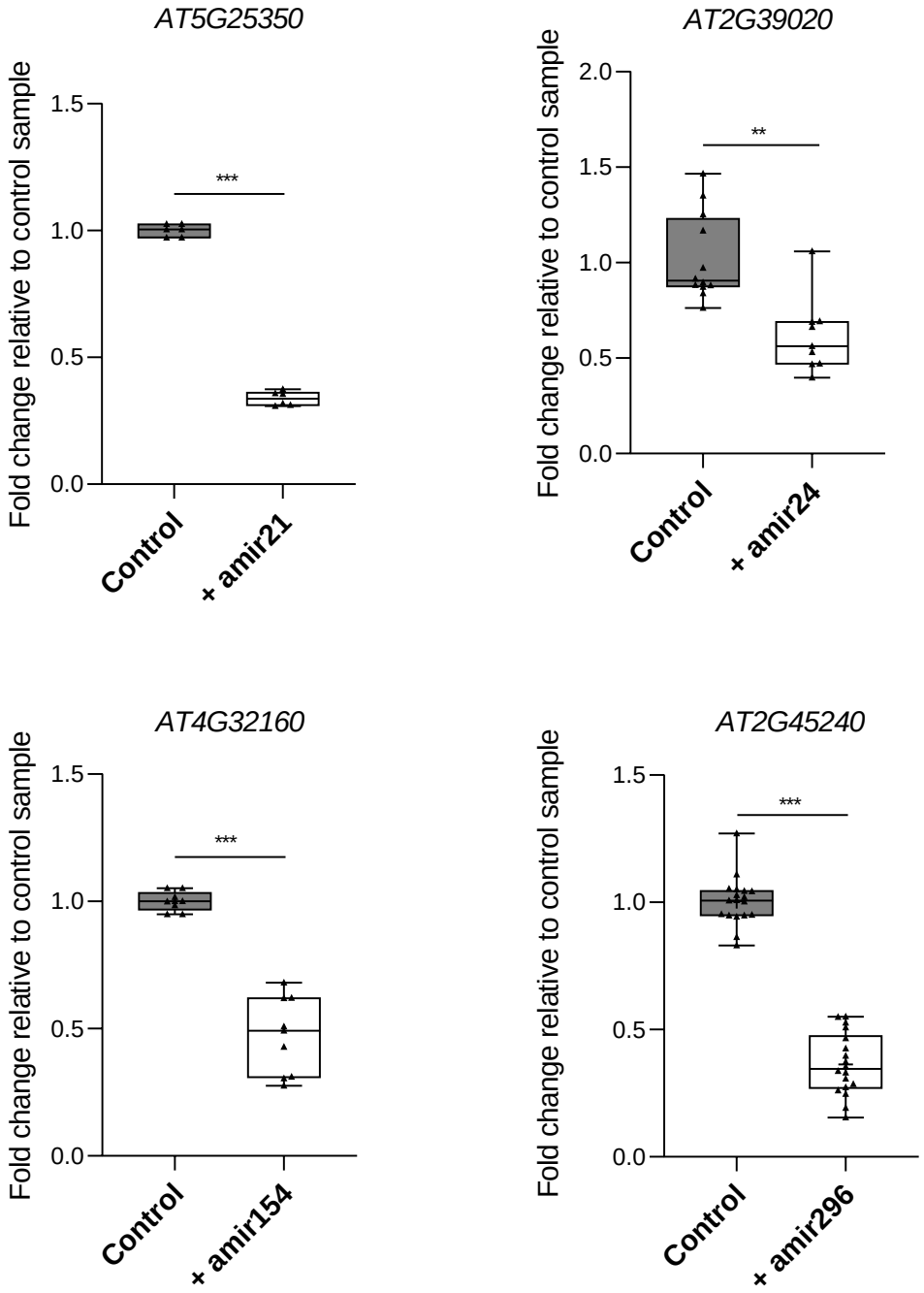

485 **Figure 8. qPCR analysis of target gene silencing in Arabidopsis protoplasts 24**
486 **h post transformation with amiRNAs.** The mRNA transcript levels in
487 transformed protoplasts (+) expressing amir21, amir24, amir154 and amir296
488 were normalized against housekeeping gene *Ubiquitin* (*AT3G62250*) and displayed
489 as fold change relative to control protoplasts (-) (mock-treated without amiRNA
490 construct). Data are the average of two to three biological replicates ± standard
491 deviation. Asterisks indicate difference at $p \leq 0.05$(*), $p \leq 0.01$ (**) and $p \leq 0.001$
492 (***) according to Student's t-test. ns= not significant.

493

494 **5'-RLM-RACE reveals canonical cleavage in protoplasts transformed with**
495 **amiRNA**

496 We selected amir296 and its predicted target gene *AT2G45240* to investigate the
497 canonical PTGS cleavage site using 5-RLM-RACE. Samples were obtained from
498 transformed protoplasts at 24 hpt, and from control samples. A distinct band of
499 approximately 383 bp was amplified from protoplasts expressing amir296,
500 consistent with the expected size of the canonical cleavage product predicted to
501 be targeted by amir296. Unexpectedly, weaker DNA fragments of a similar size
502 were detected in both control and non-treated protoplasts (Figure 9A). Cloning
503 and subsequent sequencing of the amplicons confirmed that all sequences
504 aligned with the *AT2G45240* sequence, and 50% of the obtained sequences from
505 protoplasts transformed with pUC18-AtMIR390a-RFP-amir296 (three of six clones)
506 exhibited the canonical cleavage site between nucleotide 10 and 11 of amir296. In
507 contrast, PCR products from control and natural protoplasts contained an
508 *AT2G45240* fragment but did not correspond to a canonical cleavage site,
509 suggesting a possible cleavage by an endogenous miRNA near the amir296
510 binding site or RNA degradation (Figure 9B).

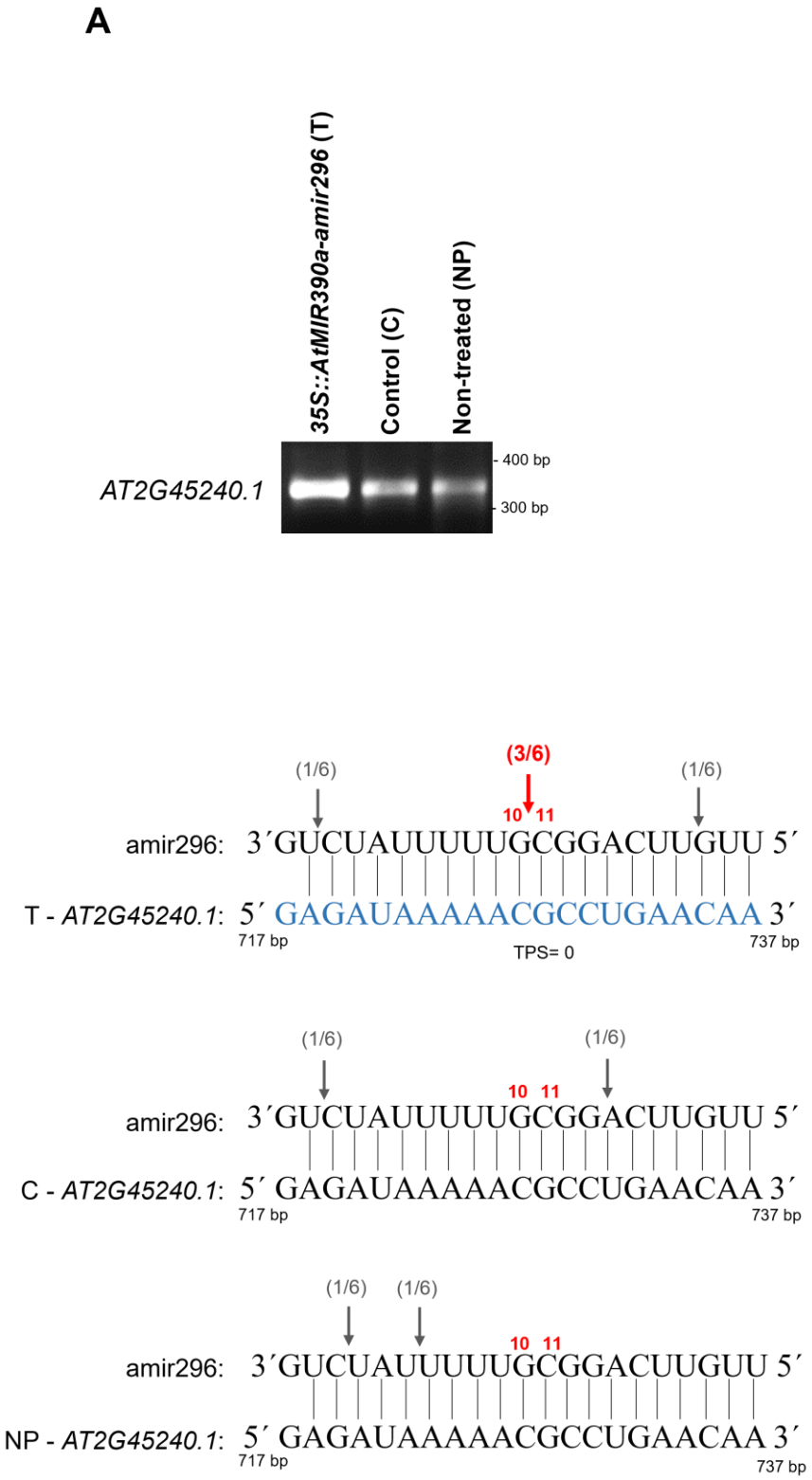

Figure 9. 5'-RLM-RACE *AT2G45240* target genes of amir296 after expression in Arabidopsis protoplasts (A) PCR products of the second nested 5´-RLM-RACE-PCR visualized in an EtBr-agarose gel. RNA was extracted from transformed

517 protoplasts with amir296 (T) and from the corresponding controls (control
518 protoplasts (C) and natural protoplasts (NP). **(B)** Mapping of *AT2G45240* target
519 cleavage products by 5´-RLM-RACE. The predicted base pairing between amir296
520 and *AT2G45240* is shown in blue. The red arrow indicates the detected canonical
521 cleavage sites. The proportion of cloned 5´-RLM-RACE products at the different
522 cleavage sites is shown in brackets. For amir296 transformed protoplasts, three
523 colonies have the 5´-end at the expected position, opposite to nucleotides 10-11
524 of amir296, which is not the case for control and non-treated protoplasts.

525 **Discussion**

526 In this work, we developed an experimental pipeline for the analysis of putative
527 fungal sRNA effectors and investigated their role in host target gene silencing. As
528 we have previously reported on the identification and analysis of fungal sRNAs
529 (*Si*sRNAs) in the interaction of *Si* and *Brachypodium distachyon* (Šečić *et al.,* 2021),
530 we aimed to bridge the gap between the large amount of bioinformatic data
531 available from this previous study, by establishing here a rapid, simple, and
532 reproducible roadmap for the analysis of *Si*sRNA effectors and their target genes
533 based on an Arabidopsis protoplast expression system. We validated the
534 effectiveness of our pipeline, by investigating sRNAs detected in the mutualistic
535 interaction between the root endophyte *Serendipita indica* and the model plant
536 *Arabidopsis thaliana* and we confirmed the accumulation of a set of *Si*sRNAs in *Si*-
537 colonized roots and their transfer to the plant cells. By immunopurification pull-
538 down assay, we showed that *Si*sRNAs are loaded into the plant RNAi machinery,
539 confirming the translocation of *Si*sRNA effectors into host cells. Using *At*AGO/sRNA
540 co-IP we detected two *Si*sRNAs, *Si*sRNA24 and *Si*sRNA28 supporting the ckRNAi
541 hypothesis. Additional *Si*sRNAs of 21 nt were identified in the *At*AGO1 Co-IP assay
542 that had some mismatches when compared to the *Si*sRNA detected in *Si* axenic
543 culture (Supplemental Table 9).

544 To gain more information about ckRNAi between *Si* and *Ath,* we generated a plant
545 expression construct under the 35S promotor for sRNA expression in protoplasts
546 based on pUC18 backbone vector and AtMIR390a distal stem-loop which can
547 generate 21 nt amiRNAs or *Si*sRNAs. The AtMIR390a precursor belongs to the
548 MIR390 family, which is highly conserved and precisely produced and processed
549 in several plant species (Axtell *et al.,* 2006; Cuperus *et al.,* 2011). Carbonell et al
550 (2014) tested the functionality of the AtMIR390a-based amiRNAs vector in
551 repressing target transcript accumulation in Arabidopsis plants using the plant
552 vector pMDC32BAtMIR390a-B/c, which enables the directed cloning of amiRNAs
553 and their stable expression in dicots plants (Carbonell *et al.,* 2014). In our
554 approach, we combined the advantages of plant expression vectors and
555 protoplast transient expression systems, both considered as valuable tools, to
556 study gene silencing and the molecular mechanisms of RNAi in plants (Tyurin *et*
557 *al.,* 2020).

558 Arabidopsis protoplasts were transformed with the putative *Si*sRNA24, and its
559 expression was validated by stem-loop PCR. Four of five predicted targets of
560 *Si*sRNA24 exhibited significantly reduced abundance in the transformed
561 protoplasts. Further analysis of the molecular cleavage pattern of *Si*sRNA24 by 5´-
562 RLM-RACE identified noncanonical cut sites in the target gene *AT4G15765.* This
563 finding may be explained by the fact that cleavage products might be present at a
564 low abundance, falling below the detection threshold of the RLM-RACE method
565 and making the detection of a precise canonical cleavage a challenge.
566 Alternatively, it might be also possible that the cleavage site within the target
567 mRNA could be located at a different position.

568 Another putative *Si*sRNA, *Si*sRNA154, which also exhibits a 5´ U and contains some
569 mismatches to two potential mRNA targets, showed a significant downregulation
570 only for the target *AT2G47600*. One major factor to consider when studying PTGS
571 via sRNA effectors is a high target predicted score (TPS) between the sRNA and

572 their predicted targets. Previous studies have demonstrated that the number and
573 position of mismatches between the sRNA and the corresponding target mRNA
574 can significantly impact their binding affinity, eventually weakening the interaction
575 and resulting in either non-significant or no downregulation (Ossowski *et al.,* 2008;
576 Rhoades *et al.,* 2002). Studies have shown that mismatches within the sRNA seed
577 region spanning nt 2 to 12/13 are possible, but they may reduce the sRNA activity,
578 whereas mismatches at position 1 or between nt 14 and 21 are more acceptable
579 (Carbonell, 2017a; Mallory *et al.*, 2004). Moreover, mismatches can also lead to a
580 different mode of action for the sRNA, and instead of an mRNA degradation
581 pathway, mismatches can trigger a deadenylation pathway or a translational
582 repression pathway, thus causing a decrease in protein synthesis instead of an
583 mRNA target degradation (Baulcombe, 2004; Carthew & Sontheimer, 2009). We
584 also hypothesize that a high abundance level of a target mRNA may lead to less
585 detectable downregulation, as its accessibility for the sRNA may have an impact
586 on the silencing process and the detection of a canonical cleavage. It is also
587 conceivable that the presence of other endogenous miRNAs, which may bind near
588 or at the same mRNA binding site might disrupt sRNA/mRNA binding, modulate
589 the regulatory outcome and affect the gene expression pattern.

590 To overcome the drawbacks of low target specificity of *Si*sRNAs, we designed
591 additional experiments based on amiRNAs with almost a perfect match to *Ath's*
592 predicted target transcript. Four amiRNAs, amir21, amir24, amir154 and amir296
593 (Supplemental Table 2), each with a 5´U were expressed in *Ath* protoplasts. All
594 amiRNAs induced a significant reduction in mRNA abundance of their
595 corresponding host-target transcripts, confirming their effective silencing activity
596 in *Ath* protoplasts.

597 Although MIR390 associates preferably with AGO7, the association of AtMIR390a-
598 derived amiRNAs that have a 5´ U is redirected to AGO1 (Carbonell, 2017b;
599 Carbonell *et al.,* 2014; Cuperus *et al.,* 2010; Montgomery *et al.,* 2008).

600 Conventionally, an sRNA-AGO1-mediated cleavage results in a canonical cut
601 between nucleotides 10 and 11 of the sRNA at the corresponding mRNA site. This
602 cleavage is a confirmation of sRNA loading into AGO1, formation of the RISC
603 complex and degradation of the mRNA target (Addo-Quaye *et al.*, 2009; Huntzinger
604 & Izaurralde, 2011). amiRNAs used in our proof of concept approach are
605 algorithmically designed to exhibit a 5' U, thereby enabling their loading into the
606 AGO1 protein (Carbonell, 2017c). Consequently, they can enter the RISC complex
607 and induce a downregulation of the target gene. Using 5'-RLM-RACE, we showed
608 that amir296 can induce a potential *At*AGO1-mediated degradation of *AT2G45240*
609 (MAP1A, METHIONINE AMINOPEPTIDASE 1A) mRNA as we detected a canonical
610 cleavage site between positions 10 and 11 of amir296 in the selected transcript.

611 Expression of all four miRNAs resulted in a significant downregulation of their
612 corresponding mRNA targets. AT5G25350 is predicted to be targeted by both
613 amir21 and *Si*sRNA21. When expressing amir21 (with 5´ U and a TPS of 0), the
614 mRNA abundance of *AT5G25350* showed a downregulation of 68%. However, when
615 expressing *Si*sRNA21 (with a 5´C and a TPS of 5) we observed a downregulation of
616 51% of the same target gene. Another example is the predicted target gene
617 *AT4G32160* targeted by amir154 and *Si*sRNA154 both with a 5´ U. The mRNA
618 abundance of *AT4G32160* in protoplasts expressing amir154 (with a TPS of 0)
619 resulted in a reduction of 50% but protoplasts expressing *Si*sRNA154 (with a TPS
620 of 4.5) did not show a reduction of *AT4G32160* transcript (Supplemental Figure 7).
621 These results raise the possibility that amiRNAs are more prone to mediate target
622 gene silencing but further studies with additional amiRNAs and putative sRNAs are
623 required to confirm these observations.

624 We also investigated whether amir296 with a 5´ U can mediate a canonical
625 cleavage of the predicted target gene *AT2G45240,* and indeed detected a cleavage
626 site of *AT2G45240* mRNA transcript between position 10 and 11 of amir296. 5´-
627 RLM-RACE is a challenging method to detect cleavage sites. High throughput

628 sequencing of samples from the *Si-Ath* interaction including transcriptional
629 analysis and degradome sequencing are needed to better understand *Si*sRNA-
630 mediated target cleavage. Moreover, consideration for sRNA non-canonical
631 cleavage site may also be further investigated as different studies speculate that
632 PTGS can still be induced through sRNA or phasiRNA and generate a non-canonical
633 cleavage site (Brousse *et al*., 2014; Ivanova *et al*., 2022).

634

635 In conclusion, we have developed a transient protoplast expression system to
636 investigate the potential role of putative *Si*sRNA effectors in regulating target gene
637 expression in *Arabidopsis thaliana* and to explore whether *Si* uses sRNAs to
638 establish a successful beneficial interaction with its host plant. This powerful
639 validation tool will not only help to understand the underlying molecular
640 mechanism of *Si*sRNA-mediated PTGS but will also allow us to examine ckRNAi in
641 mutualistic plant-fungal association.

642 By studying *Si*sRNA-mediated PTGS, we have gained valuable insights into the
643 possibility that the endophytic fungus *Si* exploits sRNA effectors for the
644 establishment of its mutualistic symbiosis with plants. More targeted studies will
645 show whether *Si* utilizes its sRNAs to potentially modulate the plant immune
646 system and identify more genes that can be silenced or upregulated during the *Si-*
647 *Ath* interaction. With the great potential of *Si* to colonize a wide host range of
648 plants, we expect that findings from the study of the *Si-Ath* interaction can be
649 translated to crop plants like barley, wheat, maize and rice. Moreover, amiRNAs
650 have been shown to be effective in fine-tuning gene expression in plants with a
651 high silencing level (Carbonell et al., 2014; Cisneros & Carbonell, 2020). Therefore,
652 they can be viewed as a potential tool for RNAi-mediated crop protection
653 strategies. Computational tools, along with *in vivo* and *in vitro* experimental setups,
654 can expand our knowledge of ckRNAi and reveal the unknown about mutualistic

655 and pathogenic interaction for cost-effective basic research and agronomic
656 application.

657 **Acknowledgements**

658 The authors gratefully thank R. Eichmann for critically reading and correcting the
659 manuscript. We thank M. Ladera-Carmona and B.T. Werner for their comments
660 and suggestions. We thank the German Research Foundation (DFG) for supporting
661 our research on RNA in plant-pathogen interactions by granting the DFG research
662 unit RU5116 on exRNA to KHK. SN is supported by the Dr. Ernst-Leopold Klipstein-
663 Stiftung, Paderborn, Giessen.

664 **Conflict of interest**

665 The authors declare that they have no competing interests.

666 **Author contributions**

667 S.N. and J.S. conceived the study; S.N. and K-H.K. wrote the paper; J.S. and E.S.
668 generated Arabidopsis target predicted genes data. S.N., K.B., and S.S. conducted
669 the functional experiments. All authors read and approved the final manuscript.

670

671

672

673

674

675

676

677

678

679

680

681

682 **References**

683 Addo-Quaye, C., Snyder, J. A., Park, Y. B., Li, Y.-F., Sunkar, R., & Axtell, M. J. (2009).
684 Sliced microRNA targets and precise loop-first processing of MIR319
685 hairpins revealed by analysis of the Physcomitrella patens degradome.
686 *RNA*, *15*(12), 2112–2121. https://doi.org/10.1261/rna.1774909
687 Adhikari, S., Turner, M., & Subramanian, S. (2013). Hairpin Priming Is Better
688 Suited than In Vitro Polyadenylation to Generate cDNA for Plant miRNA
689 qPCR. *Molecular Plant*, *6*(1), 229–231. https://doi.org/10.1093/mp/sss106
690 Akum, F. N., Steinbrenner, J., Biedenkopf, D., Imani, J., & Kogel, K.-H. (2015). The
691 Piriformospora indica effector PIIN_08944 promotes the mutualistic
692 Sebacinalean symbiosis. *Frontiers in Plant Science*, *6*, 906.
693 https://doi.org/10.3389/fpls.2015.00906
694 Axtell, M. J., Jan, C., Rajagopalan, R., & Bartel, D. P. (2006). A Two-Hit Trigger for
695 siRNA Biogenesis in Plants. *Cell*, *127*(3), 565–577.
696 https://doi.org/10.1016/j.cell.2006.09.032
697 Bargmann, B. O. R., & Birnbaum, K. D. (2009). Positive Fluorescent Selection
698 Permits Precise, Rapid, and In-Depth Overexpression Analysis in Plant
699 Protoplasts. *Plant Physiology*, *149*(3), 1231–1239.
700 https://doi.org/10.1104/pp.108.133975
701 Baulcombe, D. (2004). RNA silencing in plants. *Nature*, *431*(7006), Article 7006.
702 https://doi.org/10.1038/nature02874

703 Brousse, C., Liu, Q., Beauclair, L., Deremetz, A., Axtell, M. J., & Bouché, N. (2014). A
704 non-canonical plant microRNA target site. *Nucleic Acids Research*, *42*(8),
705 5270–5279. https://doi.org/10.1093/nar/gku157
706 Cai, Q., Qiao, L., Wang, M., He, B., Lin, F.-M., Palmquist, J., Huang, S.-D., & Jin, H.
707 (2018). Plants send small RNAs in extracellular vesicles to fungal pathogen
708 to silence virulence genes. *Science (New York, N.Y.)*, *360*(6393), 1126–1129.
709 https://doi.org/10.1126/science.aar4142
710 Carbonell, A. (2017a). Artificial small RNA-based strategies for effective and
711 specific gene silencing in plants. *Plant Gene Silencing: Mechanisms and*
712 *Applications*, 110–127. https://doi.org/10.1079/9781780647678.0110
713 Carbonell, A. (2017b). Immunoprecipitation and High-Throughput Sequencing of
714 ARGONAUTE-Bound Target RNAs from Plants. In A. Carbonell (Ed.), *Plant*
715 *Argonaute Proteins: Methods and Protocols* (pp. 93–112). Springer.
716 https://doi.org/10.1007/978-1-4939-7165-7_6
717 Carbonell, A. (2017c). Plant ARGONAUTEs: Features, Functions, and Unknowns. In
718 A. Carbonell (Ed.), *Plant Argonaute Proteins: Methods and Protocols* (pp. 1–
719 21). Springer. https://doi.org/10.1007/978-1-4939-7165-7_1
720 Carbonell, A., Takeda, A., Fahlgren, N., Johnson, S. C., Cuperus, J. T., & Carrington,
721 J. C. (2014). New generation of artificial MicroRNA and synthetic trans-
722 acting small interfering RNA vectors for efficient gene silencing in
723 Arabidopsis. *Plant Physiology*, *165*(1), 15–29.
724 https://doi.org/10.1104/pp.113.234989

725 Carthew, R. W., & Sontheimer, E. J. (2009). Origins and Mechanisms of miRNAs
726 and siRNAs. *Cell*, *136*(4), 642–655. https://doi.org/10.1016/j.cell.2009.01.035
727 Cisneros, A. E., & Carbonell, A. (2020). Artificial Small RNA-Based Silencing Tools
728 for Antiviral Resistance in Plants. *Plants*, *9*(6), Article 6.
729 https://doi.org/10.3390/plants9060669
730 Colombo, S., Nielsen, H. M., & Foged, C. (2013). Evaluation of carrier-mediated
731 siRNA delivery: Lessons for the design of a stem-loop qPCR-based
732 approach for quantification of intracellular full-length siRNA. *Journal of*
733 *Controlled Release*, *166*(3), 220–226.
734 https://doi.org/10.1016/j.jconrel.2013.01.006
735 Cuperus, J. T., Carbonell, A., Fahlgren, N., Garcia-Ruiz, H., Burke, R. T., Takeda, A.,
736 Sullivan, C. M., Gilbert, S. D., Montgomery, T. A., & Carrington, J. C. (2010).
737 Unique Functionality of 22 nt miRNAs in Triggering RDR6-Dependent siRNA
738 Biogenesis from Target Transcripts in Arabidopsis. *Nature Structural &*
739 *Molecular Biology*, *17*(8), 997–1003. https://doi.org/10.1038/nsmb.1866
740 Cuperus, J. T., Fahlgren, N., & Carrington, J. C. (2011). Evolution and Functional
741 Diversification of MIRNA Genes. *The Plant Cell*, *23*(2), 431–442.
742 https://doi.org/10.1105/tpc.110.082784
743 Derbyshire, M., Mbengue, M., Barascud, M., Navaud, O., & Raffaele, S. (2019).
744 Small RNAs from the plant pathogenic fungus Sclerotinia sclerotiorum
745 highlight host candidate genes associated with quantitative disease

746 resistance. *Molecular Plant Pathology*, *20*(9), 1279–1297.
747 https://doi.org/10.1111/mpp.12841
748 Dunker, F., Lederer, B., & Weiberg, A. (2021). Plant ARGONAUTE Protein
749 Immunopurification for Pathogen Cross Kingdom Small RNA Analysis. *Bio-*
750 *Protocol*, *11*(3), e3911. https://doi.org/10.21769/BioProtoc.3911
751 Fahlgren, N., Hill, S. T., Carrington, J. C., & Carbonell, A. (2016). P-SAMS: A web site
752 for plant artificial microRNA and synthetic trans-acting small interfering
753 RNA design. *Bioinformatics*, *32*(1), 157–158.
754 https://doi.org/10.1093/bioinformatics/btv534
755 Glaeser, S. P., Imani, J., Alabid, I., Guo, H., Kumar, N., Kämpfer, P., Hardt, M., Blom,
756 J., Goesmann, A., Rothballer, M., Hartmann, A., & Kogel, K.-H. (2016). Non-
757 pathogenic Rhizobium radiobacter F4 deploys plant beneficial activity
758 independent of its host Piriformospora indica. *The ISME Journal*, *10*(4), 871–
759 884. https://doi.org/10.1038/ismej.2015.163
760 Göhre, V., & Weiberg, A. (2023). RNA Dialogues in Fungal–Plant Relationships. In
761 B. Scott & C. Mesarich (Eds.), *Plant Relationships: Fungal-Plant Interactions*
762 (pp. 31–51). Springer International Publishing. https://doi.org/10.1007/978-
763 3-031-16503-0_2
764 He, B., Cai, Q., Qiao, L., Huang, C.-Y., Wang, S., Miao, W., Ha, T., Wang, Y., & Jin, H.
765 (2021). RNA-binding proteins contribute to small RNA loading in plant
766 extracellular vesicles. *Nature Plants*, *7*(3), 342–352.
767 https://doi.org/10.1038/s41477-021-00863-8

He, B., Hamby, R., & Jin, H. (2021). Plant extracellular vesicles: Trojan horses of cross-kingdom warfare. *FASEB BioAdvances*, *3*(9), 657–664. https://doi.org/10.1096/fba.2021-00040

Huang, G., Allen, R., Davis, E. L., Baum, T. J., & Hussey, R. S. (2006). Engineering broad root-knot resistance in transgenic plants by RNAi silencing of a conserved and essential root-knot nematode parasitism gene. *Proceedings of the National Academy of Sciences*, *103*(39), 14302–14306. https://doi.org/10.1073/pnas.0604698103

Huntzinger, E., & Izaurralde, E. (2011). Gene silencing by microRNAs: Contributions of translational repression and mRNA decay. *Nature Reviews Genetics*, *12*(2), Article 2. https://doi.org/10.1038/nrg2936

Ivanova, Z., Minkov, G., Gisel, A., Yahubyan, G., Minkov, I., Toneva, V., & Baev, V. (2022). The Multiverse of Plant Small RNAs: How Can We Explore It? *International Journal of Molecular Sciences*, *23*(7), 3979. PubMed. https://doi.org/10.3390/ijms23073979

Iwakawa, H., & Tomari, Y. (2022). Life of RISC: Formation, action, and degradation of RNA-induced silencing complex. *Molecular Cell*, *82*(1), 30–43. https://doi.org/10.1016/j.molcel.2021.11.026

Koch, A., Kumar, N., Weber, L., Keller, H., Imani, J., & Kogel, K.-H. (2013). Host-induced gene silencing of cytochrome P450 lanosterol C14α-demethylase–encoding genes confers strong resistance to Fusarium species. *Proceedings*

789 *of the National Academy of Sciences*, *110*(48), 19324–19329.
790 https://doi.org/10.1073/pnas.1306373110
791 Kramer, M. F. (2011). STEM-LOOP RT-qPCR for miRNAS. *Current Protocols in*
792 *Molecular Biology / Edited by Frederick M. Ausubel … [et Al.]*, *CHAPTER*,
793 Unit15.10. https://doi.org/10.1002/0471142727.mb1510s95
794 Lincoln, C., Britton, J. H., & Estelle, M. (1990). Growth and development of the
795 axr1 mutants of Arabidopsis. *The Plant Cell*, *2*(11), 1071–1080.
796 Liu, S., Jaouannet, M., Dempsey, D. A., Imani, J., Coustau, C., & Kogel, K.-H. (2020).
797 RNA-based technologies for insect control in plant production.
798 *Biotechnology Advances*, *39*, 107463.
799 https://doi.org/10.1016/j.biotechadv.2019.107463
800 Llave, C., Xie, Z., Kasschau, K. D., & Carrington, J. C. (2002). Cleavage of Scarecrow-
801 like mRNA Targets Directed by a Class of Arabidopsis miRNA. *Science*,
802 *297*(5589), 2053–2056. https://doi.org/10.1126/science.1076311
803 Mahanty, B., Mishra, R., & Joshi, R. K. (2023). Cross-kingdom small RNA
804 communication between plants and fungal phytopathogens-recent
805 updates and prospects for future agriculture. *RNA Biology*, *20*(1), 109–119.
806 https://doi.org/10.1080/15476286.2023.2195731
807 Mallory, A. C., Reinhart, B. J., Jones-Rhoades, M. W., Tang, G., Zamore, P. D.,
808 Barton, M. K., & Bartel, D. P. (2004). MicroRNA control of PHABULOSA in
809 leaf development: Importance of pairing to the microRNA 5' region. *The*

810 *EMBO Journal*, *23*(16), 3356–3364.
811 https://doi.org/10.1038/sj.emboj.7600340
812 Meyers, B. C., & Axtell, M. J. (2019). MicroRNAs in Plants: Key Findings from the
813 Early Years. *The Plant Cell*, *31*(6), 1206–1207.
814 https://doi.org/10.1105/tpc.19.00310
815 Mi, S., Cai, T., Hu, Y., Chen, Y., Hodges, E., Ni, F., Wu, L., Li, S., Zhou, H., Long, C.,
816 Chen, S., Hannon, G. J., & Qi, Y. (2008). Sorting of Small RNAs into
817 Arabidopsis Argonaute Complexes Is Directed by the 5' Terminal
818 Nucleotide. *Cell*, *133*(1), 116–127. https://doi.org/10.1016/j.cell.2008.02.034
819 Montgomery, T. A., Howell, M. D., Cuperus, J. T., Li, D., Hansen, J. E., Alexander, A.
820 L., Chapman, E. J., Fahlgren, N., Allen, E., & Carrington, J. C. (2008).
821 Specificity of ARGONAUTE7-miR390 interaction and dual functionality in
822 TAS3 trans-acting siRNA formation. *Cell*, *133*(1), 128–141.
823 https://doi.org/10.1016/j.cell.2008.02.033
824 Nasfi, S., & Kogel, K.-H. (2022). Packaged or unpackaged: Appearance and
825 transport of extracellular noncoding RNAs in the plant apoplast. *ExRNA; Vol*
826 *4 (May 31, 2022): ExRNA*. https://exrna.amegroups.com/article/view/64855
827 Nowara, D., Gay, A., Lacomme, C., Shaw, J., Ridout, C., Douchkov, D., Hensel, G.,
828 Kumlehn, J., & Schweizer, P. (2010). HIGS: Host-Induced Gene Silencing in
829 the Obligate Biotrophic Fungal Pathogen *Blumeria graminis*. *The Plant Cell*,
830 *22*(9), 3130–3141. https://doi.org/10.1105/tpc.110.077040

831 Osborne, R., Rehneke, L., Lehmann, S., Roberts, J., Altmann, M., Altmann, S.,
832 Zhang, Y., Köpff, E., Dominguez-Ferreras, A., Okechukwu, E., Sergaki, C.,
833 Rich-Griffin, C., Ntoukakis, V., Eichmann, R., Shan, W., Falter-Braun, P., &
834 Schäfer, P. (2023). Symbiont-host interactome mapping reveals effector-
835 targeted modulation of hormone networks and activation of growth
836 promotion. *Nature Communications*, *14*(1), Article 1.
837 https://doi.org/10.1038/s41467-023-39885-5
838 Ossowski, S., Schwab, R., & Weigel, D. (2008). Gene silencing in plants using
839 artificial microRNAs and other small RNAs. *The Plant Journal*, *53*(4), 674–
840 690. https://doi.org/10.1111/j.1365-313X.2007.03328.x
841 Qiang, X., Weiss, M., Kogel, K.-H., & Schäfer, P. (2012). Piriformospora indica—A
842 mutualistic basidiomycete with an exceptionally large plant host range.
843 *Molecular Plant Pathology*, *13*(5), 508–518. https://doi.org/10.1111/j.1364-
844 3703.2011.00764.x
845 Qiao, S. A., Gao, Z., & Roth, R. (2023). A perspective on cross-kingdom RNA
846 interference in mutualistic symbioses. *New Phytologist*, *240*(1), 68–79.
847 https://doi.org/10.1111/nph.19122
848 Reinhart, B. J., Weinstein, E. G., Rhoades, M. W., Bartel, B., & Bartel, D. P. (2002).
849 MicroRNAs in plants. *Genes & Development*, *16*(13), 1616–1626.
850 https://doi.org/10.1101/gad.1004402

851 Ren, B., Wang, X., Duan, J., & Ma, J. (2019). Rhizobial tRNA-derived small RNAs are
852 signal molecules regulating plant nodulation. *Science (New York, N.Y.)*,
853 *365*(6456), 919–922. https://doi.org/10.1126/science.aav8907
854 Rhoades, M. W., Reinhart, B. J., Lim, L. P., Burge, C. B., Bartel, B., & Bartel, D. P.
855 (2002). Prediction of Plant MicroRNA Targets. *Cell*, *110*(4), 513–520.
856 https://doi.org/10.1016/S0092-8674(02)00863-2
857 Rutter, B. D., & Innes, R. W. (2018). Extracellular vesicles as key mediators of
858 plant–microbe interactions. *Current Opinion in Plant Biology*, *44*, 16–22.
859 https://doi.org/10.1016/j.pbi.2018.01.008
860 Sang, H., & Kim, J.-I. (2020). Advanced strategies to control plant pathogenic fungi
861 by host-induced gene silencing (HIGS) and spray-induced gene silencing
862 (SIGS). *Plant Biotechnology Reports*, *14*(1), 1–8.
863 https://doi.org/10.1007/s11816-019-00588-3
864 Šečić, E., Zanini, S., Wibberg, D., Jelonek, L., Busche, T., Kalinowski, J., Nasfi, S.,
865 Thielmann, J., Imani, J., Steinbrenner, J., & Kogel, K.-H. (2021). A novel plant-
866 fungal association reveals fundamental sRNA and gene expression
867 reprogramming at the onset of symbiosis. *BMC Biology*, *19*(1), 171.
868 https://doi.org/10.1186/s12915-021-01104-2
869 Silvestri, A., Fiorilli, V., Miozzi, L., Accotto, G. P., Turina, M., & Lanfranco, L. (2019).
870 In silico analysis of fungal small RNA accumulation reveals putative plant
871 mRNA targets in the symbiosis between an arbuscular mycorrhizal fungus

872 and its host plant. *BMC Genomics*, *20*, 169. https://doi.org/10.1186/s12864-
873 019-5561-0
874 Takeda, A., Iwasaki, S., Watanabe, T., Utsumi, M., & Watanabe, Y. (2008). The
875 Mechanism Selecting the Guide Strand from Small RNA Duplexes is
876 Different Among Argonaute Proteins. *Plant and Cell Physiology*, *49*(4), 493–
877 500. https://doi.org/10.1093/pcp/pcn043
878 Tyurin, A. A., Suhorukova, A. V., Kabardaeva, K. V., & Goldenkova-Pavlova, I. V.
879 (2020). Transient Gene Expression is an Effective Experimental Tool for the
880 Research into the Fine Mechanisms of Plant Gene Function: Advantages,
881 Limitations, and Solutions. *Plants*, *9*(9), 1187.
882 https://doi.org/10.3390/plants9091187
883 Ueno, D., Yamasaki, S., & Kato, K. (2022). Methods for detecting RNA degradation
884 intermediates in plants. *Plant Science*, *318*, 111241.
885 https://doi.org/10.1016/j.plantsci.2022.111241
886 Varkonyi-Gasic, E., & Hellens, R. P. (2011). Quantitative stem-loop RT-PCR for
887 detection of microRNAs. *Methods in Molecular Biology (Clifton, N.J.)*, *744*,
888 145–157. https://doi.org/10.1007/978-1-61779-123-9_10
889 Verma, N., Narayan, O. P., Prasad, D., Jogawat, A., Panwar, S. L., Dua, M., & Johri,
890 A. K. (2022). Functional characterization of a high-affinity iron transporter
891 (PiFTR) from the endophytic fungus Piriformospora indica and its role in
892 plant growth and development. *Environmental Microbiology*, *24*(2), 689–706.
893 https://doi.org/10.1111/1462-2920.15659

894 Verma, S., Varma, A., Rexer, K.-H., Hassel, A., Kost, G., Sarbhoy, A., Bisen, P.,
895 Bütehorn, B., & Franken, P. (1998). Piriformospora indica, gen. Et sp. Nov.,
896 a new root-colonizing fungus. *Mycologia*, *90*(5), 896–903.
897 https://doi.org/10.1080/00275514.1998.12026983
898 Wang, M., Thomas, N., & Jin, H. (2017). Cross-kingdom RNA trafficking and
899 environmental RNAi for powerful innovative pre- and post-harvest plant
900 protection. *Current Opinion in Plant Biology*, *38*, 133–141.
901 https://doi.org/10.1016/j.pbi.2017.05.003
902 Wang, M., Weiberg, A., Lin, F.-M., Thomma, B. P. H. J., Huang, H.-D., & Jin, H.
903 (2016). Bidirectional cross-kingdom RNAi and fungal uptake of external
904 RNAs confer plant protection. *Nature Plants*, *2*(10), Article 10.
905 https://doi.org/10.1038/nplants.2016.151
906 Weiberg, A., Wang, M., Lin, F.-M., Zhao, H., Zhang, Z., Kaloshian, I., Huang, H.-D., &
907 Jin, H. (2013). Fungal small RNAs suppress plant immunity by hijacking host
908 RNA interference pathways. *Science (New York, N.Y.)*, *342*(6154), 118–123.
909 https://doi.org/10.1126/science.1239705
910 Weiß, M., Waller, F., Zuccaro, A., & Selosse, M.-A. (2016). Sebacinales – one
911 thousand and one interactions with land plants. *New Phytologist*, *211*(1),
912 20–40. https://doi.org/10.1111/nph.13977
913 Werner, B. T., Koch, A., Šečić, E., Engelhardt, J., Jelonek, L., Steinbrenner, J., &
914 Kogel, K.-H. (2021). Fusarium graminearum DICER-like-dependent sRNAs

915 are required for the suppression of host immune genes and full virulence.
916 *PLOS ONE*, *16*(8), e0252365. https://doi.org/10.1371/journal.pone.0252365
917 Wong-Bajracharya, J., Singan, V. R., Monti, R., Plett, K. L., Ng, V., Grigoriev, I. V.,
918 Martin, F. M., Anderson, I. C., & Plett, J. M. (2022). The ectomycorrhizal
919 fungus Pisolithus microcarpus encodes a microRNA involved in cross-
920 kingdom gene silencing during symbiosis. *Proceedings of the National*
921 *Academy of Sciences of the United States of America*, *119*(3), e2103527119.
922 https://doi.org/10.1073/pnas.2103527119
923 Wu, F.-H., Shen, S.-C., Lee, L.-Y., Lee, S.-H., Chan, M.-T., & Lin, C.-S. (2009). Tape-
924 Arabidopsis Sandwich—A simpler Arabidopsis protoplast isolation
925 method. *Plant Methods*, *5*(1), 16. https://doi.org/10.1186/1746-4811-5-16
926 Xu, L., Wu, C., Oelmüller, R., & Zhang, W. (2018). Role of Phytohormones in
927 Piriformospora indica-Induced Growth Promotion and Stress Tolerance in
928 Plants: More Questions Than Answers. *Frontiers in Microbiology*, *9*.
929 https://www.frontiersin.org/articles/10.3389/fmicb.2018.01646
930 Yoo, S.-D., Cho, Y.-H., & Sheen, J. (2007). Arabidopsis mesophyll protoplasts: A
931 versatile cell system for transient gene expression analysis. *Nature*
932 *Protocols*, *2*(7), 1565–1572. https://doi.org/10.1038/nprot.2007.199
933 Zand Karimi, H., & Innes, R. W. (2022). Molecular mechanisms underlying host-
934 induced gene silencing. *The Plant Cell*, *34*(9), 3183–3199.
935 https://doi.org/10.1093/plcell/koac165

936 Zhan, J., & Meyers, B. C. (2023). Plant Small RNAs: Their Biogenesis, Regulatory
937 Roles, and Functions. *Annual Review of Plant Biology*, *74*(1), 21–51.
938 https://doi.org/10.1146/annurev-arplant-070122-035226
939 Zhang, T., Zhao, Y.-L., Zhao, J.-H., Wang, S., Jin, Y., Chen, Z.-Q., Fang, Y.-Y., Hua, C.-
940 L., Ding, S.-W., & Guo, H.-S. (2016). Cotton plants export microRNAs to
941 inhibit virulence gene expression in a fungal pathogen. *Nature Plants*, *2*(10),
942 16153. https://doi.org/10.1038/nplants.2016.153
943 Zuccaro, A., Lahrmann, U., Güldener, U., Langen, G., Pfiffi, S., Biedenkopf, D.,
944 Wong, P., Samans, B., Grimm, C., Basiewicz, M., Murat, C., Martin, F., &
945 Kogel, K.-H. (2011). Endophytic Life Strategies Decoded by Genome and
946 Transcriptome Analyses of the Mutualistic Root Symbiont Piriformospora
947 indica. *PLOS Pathogens*, *7*(10), e1002290.
948 https://doi.org/10.1371/journal.ppat.1002290
949